

Ruthenium(II) alkynyl-hydride and ruthenium(II) bis(σ -pyridylacetylide) as ligands and linkers for metal–metal-bonded complexes

Jing-Lin Zuo,^a Eberhardt Herdtweck,^a Fabrizia Fabrizi de Biani,^{b,c} Ana M. Santos^{a,c} and Fritz E. Kühn^{*a}

^a Anorganisch-Chemisches Institut der Technischen Universität München, Lichtenbergstraße 4, D-85747 Garching bei München, Germany. E-mail: fritz.kuehn@ch.tum.de

^b Dipartimento di Chimica dell'Università di Siena, Via Aldo Moro, 53100 Siena, Italy

^c Instituto de Tecnologia Química e Biológica da Universidade Nova de Lisboa, Quinta do Marquês, EAN, Apt 127, 2781-901 Oeiras, Portugal

Received (in London, UK) 23rd January 2002, Accepted 18th April 2002

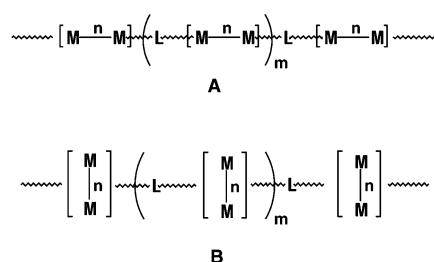
First published as an Advance Article on the web 10th June 2002

The syntheses of new linear π -conjugated building blocks, ruthenium(II) alkynyl-hydride and bis(σ -pyridylacetylide) complexes, and their application to the formation of heterobimetallic units and oligomers incorporating metal–metal-bonded complexes are reported. The structure of a tetrametallic subunit has been determined by X-ray crystallography. Thermogravimetry shows a stabilization of the tetramer and the oligomers in comparison to the least stable starting material. Spectroscopic results and cyclovoltammetry indicate an N–M donor–acceptor interaction, but no extended electron delocalization along the backbone of the tetramer.

Introduction

The development of molecular rods and wires has attracted considerable attention due to their potential applications in the rapidly emerging field of molecular electronics and devices.^{1,2} In particular, polymers and oligomers of complexes with metal–metal bonds and organic bridging ligands as building blocks for new oligomers/polymers may display novel conductive, magnetic, optical and catalytic properties.^{3,4} Two general types of one-dimensional polymers, depicted in Scheme 1, can be envisaged.

In type A, the M–M axis associated with the M–M bond is parallel to the propagating axis,⁵ whereas in type B, the M–M bond is perpendicular to the propagating axis.⁶ Oligomers and polymers of type A can be generated by axial coordination of the linking ligands to the bimetallic complexes. A variety of bimetallic centres (M–M) equatorial ligands and axial linkages (L) have been used and reported. However, the vast majority of the published work is solely based on purely organic linkers, whose effects on the metal–metal bond have been extensively examined in recent years.^{4,7,8} Organometallic bridges, however, would substantially widen the variety of available complexes and an almost unlimited combination of chain subunits would become available, awaiting novel applications.



Scheme 1

The few oligomers/polymers with organometallic linkers between metal–metal-bonded complexes usually suffer from low thermal stability or either insolubility or instability in organic donor solvents.⁹ Here, we report on a new class of oligomeric complexes of this type which are thermally quite stable, and some tetrametallic model compounds soluble without decomposition in several organic solvents. The ruthenium(II) hydride σ -pyridylacetylide complex *trans*-Ru(dppe)₂H(C≡Cpy-4) (**1**) [dppe = 1,2-bis(diphenylphosphino)ethane; C≡Cpy-4 = 4-ethynylpyridyl] and the bis(σ -pyridylacetylide) complex *trans*-Ru(dmpe)₂(C≡Cpy-4)₂ (**2**) [dmpe = 1,2-bis(dimethylphosphino)ethane] are employed as rigid-rod building blocks for the assembly of linear tetranuclear model complexes as well as oligomers.

Results and discussion

Synthesis and characterization of the ruthenium building blocks **1** and **2**

trans-Ru(dppe)₂H(C≡Cpy-4) (**1**) is a yellow solid that is readily prepared from the reaction of *cis*-Ru(dppe)₂Cl₂ with sodium and 4-ethynylpyridine in methanol (eqn. 1). This is a convenient and effective route to hydride-acetylide complexes, which are assumed to be important intermediates in the process of alkyne–vinylidene tautomerization promoted by transition metal complexes.^{10,11} The H[−] and alkynyl groups are *trans*-disposed, as evidenced by a singlet in the ³¹P{¹H} NMR spectrum (δ = 67.7 ppm). The ¹H NMR spectrum confirms the presence of the hydride ligand, showing a quintet at δ = −9.71 ppm with *J*_{PH} = 22.0 Hz. The C≡C and Ru–H stretching frequencies of **1** are located at 2055 and 1823 cm^{−1}, respectively.

Using a less bulky ligand, dmpe, the bis(acetylide) complex **2** was synthesized from [Ru(dmpe)₂H₂] by reaction with 4-ethynylpyridine (eqn. 2). It displays a sharp singlet resonance at

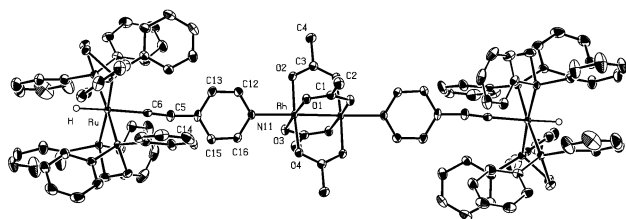
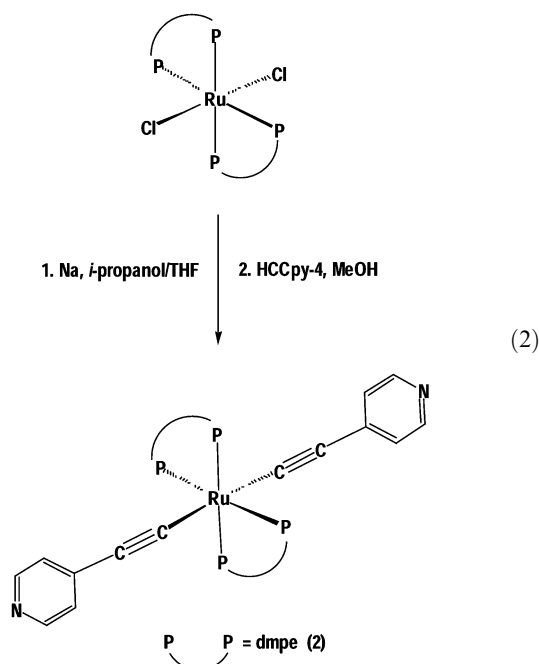
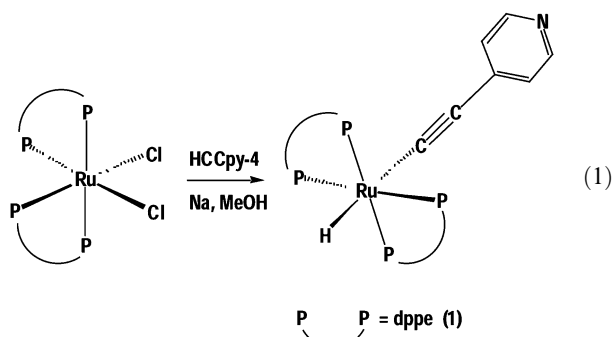


Fig. 1 ORTEP plot of complex **3** in the mixed single crystal $\{[(C_{126}H_{116}N_2O_8P_8Rh_2Ru_2)H_{1.82}/Cl_{0.18}] \cdot 3.764 CHCl_3\}$ in the solid state. Thermal ellipsoids are given at the 50% probability level. Hydrogen atoms (except for the metal-bonded hydrides) are omitted for clarity. Compound **3** is arranged around a crystallographic center of symmetry.

$\delta_P = 38.9$ ppm, confirming that the pyridylacetylide ligands adopt a *trans* configuration at the ruthenium centre. The resonance of the metal-bound carbon in the acetylide ligand appears at $\delta_C = 138.2$ ppm. The stretching frequency of the C \equiv C bond is located at 2052 cm^{-1} . Complex **2** is an excellent bidentate linear bridge for the formation of polymeric metal complexes.

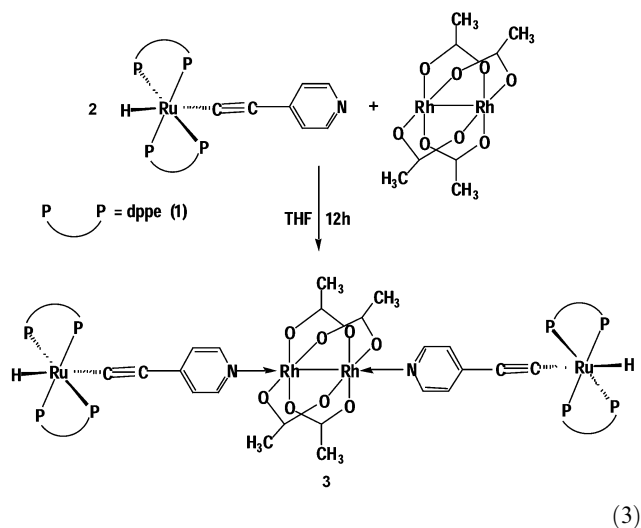


Synthesis and characterization of the tetranuclear model complex **3**

The axially ligated tetranuclear complex **3** was prepared starting from compound **1** and $Rh_2(O_2CCH_3)_4$ (eqn. 3). The hydride ligand gives rise to a quintet at $\delta_H = -9.82$ ppm with $J_{PH} = 19.0$ Hz. The pyridyl protons of complex **3**

[$\delta(H_\alpha) = 8.99$, $\delta(H_\beta) = 7.18$ ppm] resonate at lower field than the pyridyl protons in compound **1** ($\delta_H = 8.31$ and 6.82 ppm, respectively). The $\nu_{C\equiv C}$ vibration, however, is only very slightly lower for derivative **3** (2051 cm^{-1}) than for uncoordinated complex **1** (2055 cm^{-1}). The symmetric vibration of the Rh–Rh bond appears at 327 cm^{-1} , shifted by 26 cm^{-1} from the analogous vibration in $Rh_2(O_2CCH_3)_4$ (353 cm^{-1}). This shows that complex **1** is acting as an electron donor in the linear tetranuclear complex. Its rigid-rod structure, together with this electron donor property and the uncoordinated pyridyl ligand, make complex **1** a useful building block for the construction of larger scale donor–acceptor systems.

The structure of compound **3** was established by X-ray crystallography. Fig. 1 illustrates the linear rigid-rod motif along the molecular axis and the coplanarity of the pyridine ring systems in the complex. Selected bond distances and angles are listed in Table 1. The hydride atom bonded to the ruthenium was found in the difference Fourier map and refined. To our knowledge, there are very few ruthenium hydride-alkynyl complexes that have been structurally characterized, and in only one of these cases was it possible to refine the hydride.¹¹ The angles along the acetylide and metal–metal propagation axes [H–Ru–C6, $178.3(15)^\circ$; Ru–C6–C5, $177.0(2)^\circ$; Rh(a)–Rh–N11, $178.61(6)^\circ$] are close to linearity, with deviations presumably arising due to packing effects. The bond lengths Ru–C6, $2.071(2)$, and C5–C6, $1.197(3)$ Å, compare well with those found in the previously described ruthenium hydride-alkynyl complexes, namely *cis*-[RuH(C \equiv CPh)(PP₃)]·C₆H₆ [PP₃ = P(CH₂CH₂PPH₂)₃] and [Cp^{*}RuH(C \equiv CCOOMe)(dippe)]·[BPh₄].¹¹ The Ru–H separation is $1.61(5)$ Å, longer than those in [RuH(C \equiv CPh)(PP₃)]·C₆H₆ [$1.57(8)$ Å] and [Cp^{*}RuH(C \equiv CCOOMe)(dippe)]·[BPh₄] (1.35 Å, not refined and therefore to be regarded with caution). The [Rh₂(O₂CCH₃)₄] unit displays nearly idealized *D*_{4h} symmetry. The observed Rh–Rh bond distance is $2.3991(2)$ Å, which is slightly longer than that in Rh₂(O₂CCH₃)₄(H₂O)₂ [$2.3855(5)$ Å], but comparable to the Rh–Rh distances found in previously described complexes, which include a variety of axial donating ligands.⁷ The Ru···Ru distance in the linear molecule **3** spans an impressive 21.83 Å (2.183 nm).



Thermogravimetry of compounds 1–3

Details concerning the measurements are given in the Experimental, the results of the TG experiments are summarized in Table 2. The complex **1** displays its first decomposition onset at 127°C . A mass loss of *ca.* 8% is observed. This could be due to the loss of the C₂(C₅H₄N) ligand, which accounts for 10.10% of the original mass. In a second, not clearly distinct decomposition step (onset at *ca.* 243°C) an additional *ca.* 20% of the original mass is lost. This second step continues

Table 1 Selected distances (Å) and angles (°) for [Rh₂(O₂CCH₃)₄][*trans*-Ru(dppe)₂H(C≡Cpy-4)]₂·3.764CHCl₃ (**3**). Symmetry transformation used to generate equivalent atoms: (a) $-x, 1-y, 2-z$

Rh–O1	2.0423(18)	Rh–O2	2.0385(19)
Rh–O3	2.0392(19)	Rh–O4	2.0327(18)
Rh–Rh(a)	2.3991(2)	Ru–P1	2.3103(7)
Ru–P2	2.3290(7)	Ru–P3	2.3419(7)
Ru–P4	2.3231(7)	Ru–C6	2.071(2)
Ru–H	1.61(5)	C5–C6	1.197(3)
Rh–N11	2.2246(18)		
<hr/>			
O1–Rh–O2	89.00(7)	O1–Rh–O3	175.99(6)
O1–Rh–O4	90.94(7)	O1–Rh–N11	92.36(7)
O1–Rh–Rh(a)	87.67(4)	O2–Rh–O3	90.40(7)
O2–Rh–O4	175.90(6)	O2–Rh–N11	93.42(7)
O2–Rh–Rh(a)	87.97(4)	O3–Rh–O4	89.38(7)
O3–Rh–N11	91.63(7)	O3–Rh–Rh(a)	88.35(4)
O4–Rh–N11	90.68(7)	O4–Rh–Rh(a)	87.93(4)
N11–Rh–Rh(a)	178.61(6)	P1–Ru–P2	81.59(2)
P2–Ru–P3	97.28(2)	P1–Ru–P4	97.36(2)
P3–Ru–P4	83.50(2)		

above 315 °C as a further unspecific, but somewhat slower, decomposition until the end of the measurement at 650 °C. The remaining mass at this temperature accounts for 57% of the original mass. All these mass losses must be due to the disintegration of the dppe ligands.

The monometallic ruthenium building block **2** is stable up to 418 °C. The replacement of the hydride ligand in complex **1** obviously changes not only the redox behaviour (see below), but also improves the complex stability significantly. Compound **2** displays only one decomposition step with a mass loss of more than 75%. This might be due to sublimation accompanied by decomposition, since the residue is also unstable and keeps losing mass with increasing temperature. At 650 °C, less than 16% of the original mass is left. Since the Ru content in complex **2** alone accounts for 16.69%, at least partial sublimation must be involved.

The thermogravimetric investigation of compound **3** shows the onset of the first detectable decomposition step at 158 °C. According to the lost mass, this step is due to the disintegration of the Ru moieties and loss of the C₂(C₅H₄N) ligands (8.3% of the total mass). In comparison to the free compound **1**, the decomposition onset is observed at a *ca.* 30 °C higher temperature, probably due to the N–Rh interaction. The breaking of the N–Rh bond very likely leads to a fast decomposition of the Ru moiety at a temperature which is already significantly above its decomposition point (127 °C). With the onset at 274 °C, the remaining compound breaks down rapidly, leading to a further undefined decomposition without any clearly pronounced decomposition steps. The last prominent decomposition step, with its onset at 274 °C, is due to the sublimation of Rh₂(O₂CCH₃)₄. The sublimation onset of

this compound has been determined to be at 278 °C.⁹ Due to the accompanying thermal breakdown of the remnants of the Ru ligand, the second decomposition step is not so clearly defined in the case of compound **3** and lasts until the end of the measurement at 650 °C.

Electrochemistry of compounds 1–3

In Table 3, the redox potentials of compounds **1–3** are collected together, Fig. 2 gives a comparison of their cyclic voltammetric responses. All the compounds undergo an oxidation process, ascribed to the Ru^{II}/Ru^{III} redox change. Substitution of the hydride by pyridylacetylide makes the redox potential of compound **2** shift anodically by 130 mV with respect to that of complex **1**. Nevertheless, the ligand substitution has a more important effect on the reversibility of the redox processes of these complexes. Indeed, as is shown in Fig. 2(a), the oxidation process of compound **1** is chemically irreversible; the complex decomposes upon removal of one electron and a new complex is formed, which undergoes oxidation at a more anodic potential. In contrast, the oxidation process of complex **2** [Fig. 2(b)] is both chemically and electrochemically reversible (i_{pc}/i_{pa} is constantly 1, $\Delta E_p = 80$ mV). A reasonable ECE mechanism for compound **1** is shown in Scheme 2.

Since the limit sensitivity of the CV technique is estimated to be around 20 mV, it can be assumed that complex **3** exhibits the same redox behaviour as compound **1**, indeed the redox potential value of the first is cathodically shifted by only 30 mV with respect to the latter and is also chemically irreversible. On the basis of the redox behaviour observed for compound **1**,

Table 2 TG data for the compounds **1–6**

Compound	First decomposition step		Second decomposition step		Residual mass at 650 °C (%)
	Onset/°C	Mass loss (%)	Onset/°C	Mass loss (%)	
1	127	8	243	20 ^a	57
2	418	75	— ^a	—	16
3	158	8	274	— ^b	40
4	299	18	— ^c	—	76
5	262	— ^b	—	—	55
6	260	30	— ^a	—	56

^a Unspecific further decomposition (without a distinct onset). ^b Clearly defined onset but continuous significant mass loss until 650 °C. ^c Minor, but continuous mass loss after the first decomposition step.

Table 3 Redox parameters for complexes 1–3

Compound	<i>E</i> /V	ΔE_p /mV
1	+0.31 ^a	—
2	+0.44	80
3	+0.28 ^{a, b}	—

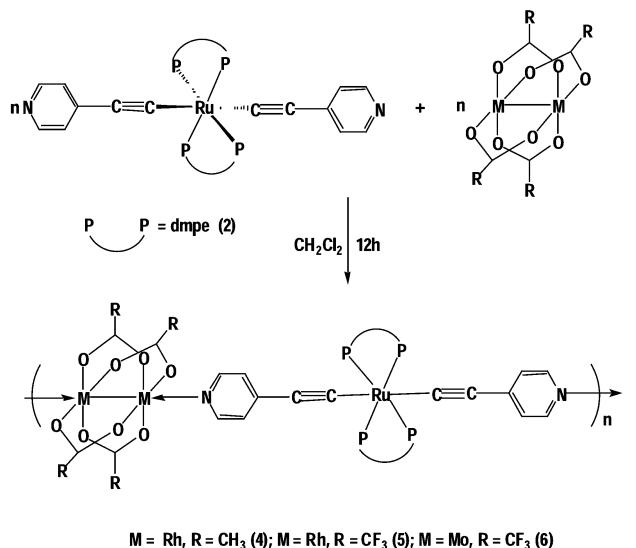
^a Peak potential for irreversible process. ^b Two-electron process, see text.

it seems reasonable to assume that the redox process observed in the symmetric dimer 3 is a two-electron process. The absence of two separate waves for the two ruthenium-based subunits strongly suggests that they are non-communicating, which is not unexpected considering the long distance between them. The usual methods to confirm this assumption beyond any doubt (bulk electrolysis and/or the addition of an equimolar amount of ferrocene to compare the peak intensities) could, unfortunately, not be applied successfully in the particular case of compound 3, due to experimental difficulties. Further work aimed at getting a clearer picture of this topic is currently under way in our laboratories.

Synthesis of oligomeric compounds

Mixing $\text{Rh}_2(\text{O}_2\text{CCH}_3)_4$, $\text{Rh}_2(\text{O}_2\text{CCF}_3)_4$ or $\text{Mo}_2(\text{O}_2\text{CCF}_3)_4$ with an equimolar amount of complex 2 in CH_2Cl_2 yields precipitates of the oligomeric metal complexes (eqn. 4), which can be easily isolated. The poor solubility of the oligomers prevents a detailed study of their properties in solution. However, the elemental analyses provide a rough way of estimating the numbers of repeating units. The analytical results for these complexes suggest that the terminal groups are bimetallic tetracarboxylates. The oligomers can be represented as $[\text{M}_2(\text{O}_2\text{CR})_4]_n + [\text{Ru}(\text{dmpe})_2(\text{C}\equiv\text{Cpy-4})_2]_n$ ($\text{M} = \text{Rh}$, $\text{R} = \text{CH}_3$, 4; $\text{M} = \text{Rh}$, $\text{R} = \text{CF}_3$, 5; $\text{M} = \text{Mo}$, $\text{R} = \text{CF}_3$, 6) and the average number of repeating units (*n*) is 7, 5 and 2 for complexes 4, 5 and 6, respectively (it is not unlikely they are mixtures of oligomers with different lengths). Complex 5 is poorly soluble in CH_2Cl_2 and its UV absorption spectrum displays the MLCT band [$\text{d}\pi_{(\text{Ru})} \rightarrow \pi^*_{(\text{C}\equiv\text{Cpy})}$] at 385 nm; in complex 2, this transition appears at 358 nm. The red shift is ascribed to the Lewis acidity of the $\text{Rh}_2(\text{O}_2\text{CCF}_3)_4$ moiety. The symmetric stretching vibrations of the metal–metal bonds in polymeric metal complexes 4, 5 and 6 appear at $\nu = 326$, 326 and 367 cm^{-1} , respectively, which are 27, 28 and 31 cm^{-1} lower than the values in the non-axial coordinated complexes. Thus, the changes are only very slightly more pronounced than

in the tetranuclear complex 3. Furthermore, the $\text{C}\equiv\text{C}$ stretching frequencies decrease significantly in the polymers, but the stretching frequencies of the pyridyl ring increase somewhat in comparison to the monomers. This observation is in accord with the electron-donating ability of the ruthenium(II) acetylide-pyridine unit, which decreases the strength of the metal–metal bonds.



(4)

Thermogravimetry of the oligomeric complexes

The decomposition of compound 4 begins at 299°C . It is therefore significantly more stable than complex 3 (see Table 2), and also still stable at the sublimation temperature of $\text{Rh}_2(\text{O}_2\text{CCH}_3)_4$ (278°C). It seems that the $\text{Rh}-\text{N}$ interactions in the oligomeric molecular rod are stable enough to hinder the sublimation of the Rh_2 building block. During the decomposition, the compound loses about 18% of its original mass. This mass loss is not high enough to assume sublimation of $\text{Rh}_2(\text{O}_2\text{CCH}_3)_4$. This would account for 45.48% of the mass of the complex 4. A (partial) loss of the acetate ligands (in total 24.30% of the original mass) seems more likely. Unfortunately, due to the insolubility of the residue left after the first decomposition step, its exact nature could not be determined. After the first decomposition step, the compound remains relatively stable up to 650°C with only a minor additional mass loss.

Interestingly, compound 5 is less stable than complex 4, despite the fact that the Rh starting material, $\text{Rh}_2(\text{O}_2\text{CCF}_3)_4$, has a higher sublimation onset than its non-fluorinated congener ($312\text{ vs. }278^\circ\text{C}$).⁹ Compound 5 starts to decompose from 262°C . In contrast to compound 4, this decomposition step is less clearly pronounced and seems to consist of some less developed “substeps” of different sizes. Whether or not this observation is due to the fact that compound 5 is a mixture of oligomers of different chain lengths cannot be definitively answered, but it seems likely. In any case, the $\text{Rh}-\text{N}$ interaction must be quite weak in this compound.

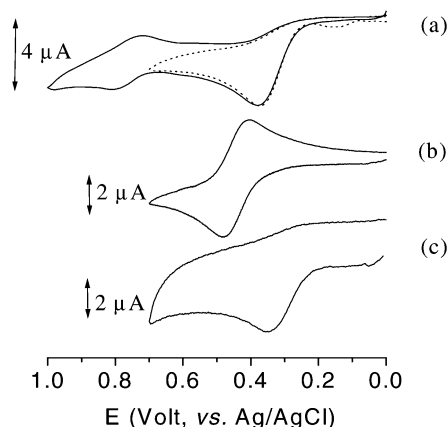
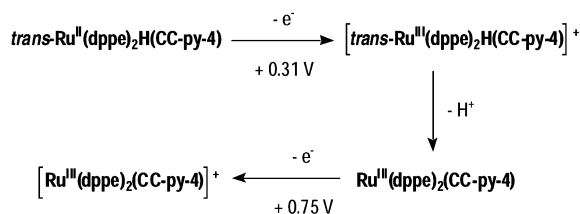


Fig. 2 Cyclic voltammograms of CH_2Cl_2 solutions of TBAH (0.2 mol dm^{-3}) and (a) 1 ($2.2 \times 10^{-4}\text{ mol dm}^{-3}$); (b) 2 ($7.2 \times 10^{-4}\text{ mol dm}^{-3}$); (c) 3 (unknown since sample not weighed). Scan rate 0.1 (a) and 0.2 Vs^{-1} (b, c). Pt (a, b) and glassy carbon (c) working electrodes.



Scheme 2

Compound **6** decomposed in a defined single step with the onset at 260 °C. The $\text{Mo}_2(\text{O}_2\text{CCF}_3)_4$ starting complex undergoes sublimation at 226 °C.⁹ Again, the oligomer remains intact at temperatures above the sublimation temperature of the $\text{Mo}(\text{II})$ starting material. Only at a temperature about 35 °C above the sublimation onset of $\text{Mo}_2(\text{O}_2\text{CCF}_3)_4$ does complex **6** start decomposing. The mass loss during the decomposition step of compound **6** accounts for *ca.* 30% of the original mass. This is significantly less than the $\text{Mo}_2(\text{O}_2\text{CCF}_3)_4$ content of the oligomer (58.72%). Probably due to the high temperature at which the Mo–N interaction breaks, only part of the $\text{Mo}_2(\text{O}_2\text{CCF}_3)_4$ sublimes, the rest decomposes. Behaviour like this is not uncommon and has been observed for some other oligomeric compounds containing sublimable building blocks.⁹

Conclusions

trans- $\text{Ru}(\text{dppe})_2\text{H}(\text{C}\equiv\text{Cpy-4})$ (**1**) [dppe = 1,2-bis(diphenylphosphino)ethane] and the bis(σ -pyridylacetylide) complex *trans*- $\text{Ru}(\text{dmpe})_2(\text{C}\equiv\text{Cpy-4})_2$ (**2**) [dmpe = 1,2-bis(dimethylphosphino)ethane] can be used as linkers for metal–metal units in heterometallic complexes. Tetranuclear model complexes of the type Ru-L-M-M-L-Ru and oligomers of the type $(\text{M-M-L-Ru-L})_n$ are accessible *via* complexes **1** and **2** and M–M units as starting materials. The product complexes are thermally quite stable and also stable to air and moisture. According to the spectroscopic results, the N–M interaction is a typical donor–acceptor interaction. Significant electron delocalization along the backbone of complex **3** is not observed. In order to obtain a detectable degree of electron delocalization, M–C interactions are the building blocks of choice.

Experimental

General procedures

The preparations and manipulations were carried out under an oxygen- and water-free argon atmosphere using standard Schlenk techniques. Solvents were dried by standard procedures, distilled and kept under argon over molecular sieves. 4-Ethynylpyridine,¹² *cis*- $\text{Ru}(\text{dppe})_2\text{Cl}_2$,¹³ $\text{Mo}_2(\text{O}_2\text{CCF}_3)_4$,¹⁴ $\text{Rh}_2(\text{O}_2\text{CCH}_3)_4$ ¹⁵ and $\text{Rh}_2(\text{O}_2\text{CCF}_3)_4$ ¹⁶ were prepared according to the literature methods. Elemental analyses were performed in the Mikroanalytisches Labor of the TU München in Garching. ¹H, ¹³C and ³¹P{¹H} NMR were obtained using a Bruker Avance DPX-400 spectrometer. IR (from KBr pellets) and Raman spectra (powder samples) were obtained on a Bio-Rad FTS-575C spectrometer at room temperature. Electronic absorption spectra were run using a Perkin-Elmer Lambda 2 UV/VIS spectrometer. Cyclic voltammograms were recorded with a computer-controlled Model 173 potentiostat/galvanostat (EG&G Princeton Applied Research) from argon-saturated dried solutions with tetrabutylammonium hexafluorophosphate (TBAH, 0.2 M) as supporting electrolyte. The working electrode was platinum or glassy carbon and the reference electrode was silver/silver chloride. TGA data were obtained using a Perkin-Elmer TGA 7 thermobalance. Each 3–10 mg sample was heated in an open crucible under a dynamic He atmosphere (purity 5.0, flow 45 sccm) using a 50–650 °C temperature program at a heating rate of 10 K min^{−1}. The samples were filled into the crucibles under a dry inert gas atmosphere.

Synthesis of the building blocks

trans- $\text{Ru}(\text{dppe})_2\text{H}(\text{C}\equiv\text{Cpy-4})$ (**1**). 4-Ethynylpyridine (103.0 mg, 1.0 mmol) was added to a solution of *cis*- $\text{Ru}(\text{dppe})_2\text{Cl}_2$ (290.6 mg, 0.30 mmol) in methanol (20 ml). Then sodium

(130 mg) was added and the mixture was refluxed for 5 h. The resulting solid was filtered off and washed with methanol and Et₂O. It was purified by recrystallization from CHCl_3 –Et₂O (Yield: 210 mg, 70%). IR (KBr, cm^{−1}): 2055, 1823, 693, 490. δ_{H} (CDCl_3 , 400 MHz): 1.96 (s, 4H, CH₂), 2.43 (s, 4H, CH₂), 6.82 (d, $J_{\text{H-H}} = 5.2$ Hz, 2H, H_B), 6.92–7.42 (m, 40H, Ph), 8.31 (d, $J_{\text{H-H}} = 5.2$ Hz, 2H, H_A), −9.71 (qn, $J_{\text{PH}} = 22.0$ Hz, 1H, RuH). δ_{C} (CDCl_3): 33.4, 125.0, 127.3, 127.4, 128.8, 129.0, 133.9, 134.0, 149.2. δ_{P} (CDCl_3): 67.7. FAB-MS m/z : 1002.8 $[\text{M} + \text{H}]^+$. Anal. calc. for $\text{C}_{59}\text{H}_{53}\text{NP}_4\text{Ru}$: C, 70.79; H, 5.33; N, 1.40; found: C, 70.45; H, 5.40; N, 1.27%.

trans- $\text{Ru}(\text{dmpe})_2(\text{C}\equiv\text{Cpy-4})_2$ (**2**). A solution of *trans*- $\text{Ru}(\text{dmpe})_2\text{Cl}_2$ (100 mg, 0.21 mmol) in 2-propanol–THF (1:9, 25 ml) was stirred for 10 min, then sodium (220 mg) was added and the solution was stirred for 30 h at room temperature. The solvent was removed *in vacuo* and the residue was extracted with n-pentane. The extracts were evaporated to dryness to afford $[\text{Ru}(\text{dmpe})_2\text{H}_2]$. The hydride complex was dissolved in MeOH and 4-ethynylpyridine (127 mg, 1.2 mmol) was added. The mixture was refluxed for 1.5 h and the solution was concentrated to 5 ml. The pale yellow solid was filtered off and washed with MeOH and Et₂O and dried *in vacuo* (Yield: 89 mg; 70%). IR (KBr, cm^{−1}): 2052, 1449, 528. δ_{H} (CD_2Cl_2 , 400 MHz): 1.55 (s, 24H, PCH₃), 1.71 (t, $J_{\text{H-H}} = 9.0$ Hz, 8H, PCH₂), 6.81 (d, $J_{\text{H-H}} = 6.0$ Hz, 4H, H_B), 8.16 (d, $J_{\text{H-H}} = 5.9$ Hz, 4H, H_A). δ_{C} (CD_2Cl_2): 15.8 (qn), 30.4 (qn), 109.0, 125.1, 138.2, 144.6, 149.3. δ_{P} (CD_2Cl_2): 38.9. FAB-MS m/z : 606.5 $[\text{M} + \text{H}]^+$. Anal. calc. for $\text{C}_{26}\text{H}_{40}\text{N}_2\text{P}_4\text{Ru}$: C, 51.57; H, 6.66; N, 4.63; found: C, 51.13; H, 6.59; N, 4.32%.

Synthesis of tetranuclear units

$[\text{Rh}_2(\text{O}_2\text{CCH}_3)_4][\text{trans-Ru}(\text{dppe})_2\text{H}(\text{C}\equiv\text{Cpy-4})_2]$ (**3**). A solution (30 ml) of **1** (200 mg, 0.20 mmol) and $\text{Rh}_2(\text{O}_2\text{CCH}_3)_4$ (42 mg, 0.095 mmol) in THF (30 ml) was stirred overnight at room temperature. The solvent was removed and the solid residue obtained was washed with EtOH and Et₂O, and dried *in vacuo* (Yield: 183 mg, 75%). Orange crystals of **3** were obtained by diffusing Et₂O into a CH_2Cl_2 – CHCl_3 solution of the complex (Yield: 97 mg; 40%). IR (KBr, cm^{−1}): 2051, 1814, 1433, 695, 530. δ_{H} (CD_2Cl_2 , 400 MHz): 1.95 (s, 12H, CH₃), 2.08 (s, 8H, PCH₂), 2.61 (t, 8H, PCH₂), 7.09–7.51 (m, 80H, Ph), 7.18 (d, 4H, H_B), 8.99 (d, 4H, H_A), −9.82 (qn, $J_{\text{PH}} = 19.0$ Hz, 1H, RuH). δ_{C} (CD_2Cl_2): 23.9, 33.5, 116.0, 126.1–139.6 (m), 149.5, 153.3, 191.5. δ_{P} (CD_2Cl_2): 67.4. Anal. calc. for $\text{C}_{126}\text{H}_{118}\text{N}_2\text{O}_8\text{P}_8\text{Rh}_2\text{Ru}_2\cdot\text{CHCl}_3$: C, 59.50; H, 4.68; N, 1.09; found: C, 59.12; H, 4.82; N, 0.91%.

Synthesis of oligomeric complexes

Compounds 4–6. 0.1 mmol of $\text{Rh}_2(\text{O}_2\text{CCH}_3)_4$, $\text{Rh}_2(\text{O}_2\text{CCF}_3)_4$ or $\text{Mo}_2(\text{O}_2\text{CCF}_3)_4$, respectively, was mixed with an equimolar amount of compound **2** in CH_2Cl_2 under a nitrogen atmosphere. The reaction mixtures were stirred overnight at room temperature. The precipitates were collected and washed with CH_2Cl_2 and Et₂O, then dried *in vacuo*. Compound **4**, $[\text{Rh}_2(\text{O}_2\text{CCH}_3)_4][\text{Ru}(\text{dmpe})_2(\text{C}\equiv\text{Cpy-4})_2]_7$, (Yield: 78 mg; 80%). IR (KBr, cm^{−1}): 2903, 2028, 1593, 1426, 1204, 696. Raman (cm^{−1}): 2909, 2065, 1598, 1209, 1015, 568, 367, 347, 326. Anal. calc. for $\text{C}_{246}\text{H}_{376}\text{N}_{14}\text{O}_{64}\text{P}_{28}\text{Rh}_{16}\text{Ru}_7$: C, 38.00; H, 4.87; N, 2.52; found: 37.63; H, 4.92; N, 2.49%. Compound **5**, $[\text{Rh}_2(\text{O}_2\text{CCF}_3)_4][\text{Ru}(\text{dmpe})_2(\text{C}\equiv\text{Cpy-4})_2]_5$, (Yield: 64 mg; 55%). IR (KBr, cm^{−1}): 2907, 2008, 1601, 1201, 737. Raman (cm^{−1}): 2057, 1605, 1206, 574, 365, 326. Anal. calc. for $\text{C}_{178}\text{H}_{200}\text{N}_{10}\text{F}_{72}\text{O}_{48}\text{P}_{20}\text{Rh}_{12}\text{Ru}_5$: C, 30.65; H, 2.89; N, 2.01; found: C, 30.64; H, 2.85; N, 2.08%. Compound **6**, $[\text{Mo}_2(\text{O}_2\text{CCF}_3)_4][\text{Ru}(\text{dmpe})_2(\text{C}\equiv\text{Cpy-4})_2]_5$, (Yield: 47 mg; 45%), IR (KBr, cm^{−1}): 2906, 2009, 1608, 1195, 730, 537.

Table 4 Crystallographic data for $[\text{Rh}_2(\text{O}_2\text{CCH}_3)_4][\text{trans-Ru}(\text{dppe})_2\text{H}(\text{C}\equiv\text{Cpy-4})]_2 \cdot 3.764\text{CHCl}_3$ (3)

Formula	$(\text{C}_{126}\text{H}_{116}\text{N}_2\text{O}_8\text{P}_8\text{Rh}_2\text{Ru}_2)\text{H}_{1.82}/\text{Cl}_{0.18} \cdot 3.764\text{CHCl}_3$
M_r	2899.50
T/K	123
$\lambda/\text{\AA}$	0.71073
Crystal system	Triclinic
Space group	$P\bar{1}$
$a/\text{\AA}$	12.6709(1)
$b/\text{\AA}$	16.4638(1)
$c/\text{\AA}$	17.1025(1)
$\alpha/^\circ$	105.3292(3)
$\beta/^\circ$	109.3507(3)
$\gamma/^\circ$	99.4126(5)
$U/\text{\AA}^3$	3120.36(4)
Z	1
μ/mm^{-1}	0.903
Reflections collected	59 877
Independent reflections	11 463 [$R_{\text{int}} = 0.031$]
Final R indices [$I > 2\sigma(I)$]	$R1 = 0.0278$, $wR2 = 0.0683$
R indices (all data)	$R1 = 0.0320$, $wR2 = 0.0709$
Goodness-of-fit parameter (GOF)	1.035

Raman (cm^{-1}): 2045, 1603, 1208, 1004, 367. Anal. calc. for $\text{C}_{76}\text{H}_{80}\text{N}_4\text{F}_{36}\text{O}_{24}\text{P}_8\text{Mo}_6\text{Ru}_2$: C, 29.04; H, 2.57; N, 1.78; found: C, 28.76; H, 3.02; N, 1.90%.

X-Ray crystallography

Single crystals of $[(\text{C}_{126}\text{H}_{116}\text{N}_2\text{O}_8\text{P}_8\text{Rh}_2\text{Ru}_2)\text{H}_{1.82}/\text{Cl}_{0.18}] \cdot 3.764\text{CHCl}_3$ were obtained as described above. The diffraction experiment was carried out at 123 K on a Kappa CCD area detecting diffraction system equipped with a rotating anode and graphite monochromated Mo-K α radiation ($\lambda = 0.71073$ Å). The unit cell parameters were obtained by full-matrix least squares refinements of 11 394 independent reflections. The structure was solved by direct methods using SIR92¹⁷ and refined by full-matrix least squares (based on F^2) using SHELXL-97.¹⁸ Non-hydrogen atoms were refined with anisotropic displacement parameters. The hydrogen atoms were placed in calculated positions ($d_{\text{C-H}} = 0.95, 0.98, 0.99, 1.00$ Å). The hydride bonded to the ruthenium atom was found in the difference Fourier map and refined freely. Table 4 lists the details of data processing and structure refinements.

Two crystallographically independent CHCl_3 solvent molecules show site occupancy factors of 0.949(2) and 0.933(2). Two of the eight phenyl groups of the dppe ligands appear to be disordered over two positions with a ratio of 74:26.

Crystals grown from a second and independent reaction pathway, and from CH_2Cl_2 , show exactly the same chlorine content and the same disorder of the phenyl groups. *Crystal data*: triclinic, space group $P\bar{1}$, $a = 9.2242(1)$, $b = 13.3295(1)$, $c = 24.4310(2)$ Å, $\alpha = 91.4546(3)$, $\beta = 95.2830(3)$, $\gamma = 105.6513(4)^\circ$, $V = 2876.27(5)$ Å³, $Z = 1$, $T = 123(1)$ K. We assume that the reaction mixture contains traces of the dichloro analogue of **3** $[(\text{C}_{126}\text{H}_{116}\text{N}_2\text{O}_8\text{P}_8\text{Rh}_2\text{Ru}_2)\text{Cl}_2]$. Both components cocrystallize as mixed single crystals.

CCDC reference number 184199. See <http://www.rsc.org/suppdata/nj/b2/b200913g/> for crystallographic data in CIF or other electronic format.

Acknowledgements

The authors are greatly indebted to Prof. W. A. Herrmann and Prof. Carlos C. Romão for their continuing support. The FCI

is acknowledged for financial support. J.-L. Z. thanks the Alexander von Humboldt Foundation for a postdoctoral research associate fellowship. A. M. S. is grateful to the PRAXIS XXI for a postdoctoral research fellowship.

References

- (a) *Molecular Electronics*, ed. J. Jortner and M. A. Ratner, Blackwell, Cambridge, 1997; (b) J. M. Lehn, *Supramolecular Chemistry: Concepts and Perspective*, VCH, Weinheim, 1995, ch. 8.
- (a) P. F. H. Schwab, M. D. Levin and J. Michl, *Chem. Rev.*, 1999, **99**, 1863; (b) R. P. Kingsborough and T. M. Swager, *Prog. Inorg. Chem.*, 1999, **48**, 123; (c) T. Ren, G. Zou and J. C. Alvarez, *Chem. Commun.*, 2000, 1197.
- (a) S. R. Marder, *Inorganic Materials*, ed. D. W. Bruce and D. O'Hare, Wiley, Chichester, 1992, 115; (b) F. A. Cotton, L. M. Daniels, C. Li, C. A. Murillo, *J. Am. Chem. Soc.*, 1999, **121**, 4538.
- M. H. Chisholm, *Acc. Chem. Res.*, 2000, **33**, 53 and references cited therein.
- (a) J. L. Wesemann and M. H. Chisholm, *Inorg. Chem.*, 1997, **36**, 3258; (b) F. A. Cotton, E. V. Dikarev, M. A. Petrukhina and S. E. Stiriba, *Inorg. Chem.*, 2000, **39**, 1748; (c) F. A. Cotton, E. V. Dikarev, M. A. Petrukhina and S. E. Stiriba, *Organometallics*, 2000, **19**, 1402; (d) K. T. Wong, J. M. Lehn, S. M. Peng and G. H. Lee, *Chem. Commun.*, 2000, 2259; (e) G. Xu and T. Ren, *Organometallics*, 2001, **20**, 2400; (f) H. Miyasaka, R. Clérac, C. S. Campos-Fernández and K. R. Dunbar, *Inorg. Chem.*, 2001, **40**, 1663; (g) L. Bear, B. Han, Z. Wu, E. van Caemelbecke and K. M. Kadish, *Inorg. Chem.*, 2001, **40**, 2275.
- (a) F. A. Cotton, C. Lin and C. A. Murillo, *J. Chem. Soc., Dalton Trans.*, 1998, 3151; (b) F. A. Cotton, L. M. Daniels, C. Lin and C. A. Murillo, *Chem. Commun.*, 1999, 841; (c) F. A. Cotton, C. Lin and C. A. Murillo, *Chem. Commun.*, 2001, 11; (d) F. A. Cotton, C. Lin and C. A. Murillo, *J. Am. Chem. Soc.*, 2001, **123**, 2670.
- F. A. Cotton and R. A. Walton, *Multiple Bonds Between Metal Atoms*, Oxford University Press, London, 2nd edn., 1993 and references cited therein.
- (a) J. L. Bear, B. Han and S. Huang, *J. Am. Chem. Soc.*, 1993, **115**, 1175; (b) F. A. Cotton and T. Ren, *Inorg. Chem.*, 1995, **34**, 3190; (c) J. L. Bear, B. Han, S. Huang and K. M. Kadish, *Inorg. Chem.*, 1996, **35**, 3012; (d) M. H. Chisholm, G. Christou, K. Foltling, J. C. Huffman, C. A. James, J. A. Samuels, J. L. Wesemann and W. H. Woodruff, *Inorg. Chem.*, 1996, **35**, 3643; (e) J. L. Bear, Y. Li, B. Han, E. van Caemelbecke and K. M. Kadish, *Inorg. Chem.*, 1997, **36**, 5449; (f) C. Lin, T. Ren, E. J. Valente and J. D. Zubowski, *J. Chem. Soc., Dalton Trans.*, 1998, 571; (g) W. M. Xue, F. E. Kühn, G. Zhang, E. Herdtweck and G. Raudaschl-Sieber, *J. Chem. Soc., Dalton Trans.*, 1999, 4103; (h) C. Lin, T. Ren, E. J. Valente and J. D. Zubowski, *J. Organomet. Chem.*, 1999, **579**, 114; (i) W. M. Xue, F. E. Kühn, G. Zhang and E. Herdtweck, *J. Organomet. Chem.*, 2000, **596**, 177; (j) G. Zou, J. C. Alvarez and T. Ren, *J. Organomet. Chem.*, 2000, **596**, 152; (k) G. Xu and T. Ren, *Inorg. Chem.*, 2001, **40**, 2925.
- (a) W. M. Xue and F. E. Kühn, *Eur. J. Inorg. Chem.*, 2001, 2041; (b) W. M. Xue, F. E. Kühn, E. Herdtweck and Q. Li, *Eur. J. Inorg. Chem.*, 2001, 213; (c) W. M. Xue, F. E. Kühn and E. Herdtweck, *Polyhedron*, 2001, **20**, 791.
- (a) M. I. Bruce, *Chem. Rev.*, 1991, **91**, 197 and references therein; (b) C. Bruneau and P. H. Dixneuf, *Acc. Chem. Res.*, 1999, **32**, 311.
- (a) I. de los Ríos, M. J. Tenorio, M. C. Puerta and P. Valerga, *J. Am. Chem. Soc.*, 1997, **119**, 6529; (b) C. Bianchini, P. Frediani, D. Masi, M. Peruzzini, F. Zanobini, *Organometallics*, 1994, **13**, 4616.
- L. O. Ciana and A. Haim, *J. Heterocycl. Chem.*, 1984, **121**, 607.
- B. Chaudret, G. Commenges and R. Poilblanc, *J. Chem. Soc., Dalton Trans.*, 1984, 1635.
- F. A. Cotton and J. G. Norman, *J. Coord. Chem.*, 1971, **1**, 161.
- G. A. Rempel, P. Legzdins, H. Smith and G. Wilkinson, *Inorg. Synth.*, 1972, **13**, 90.
- J. Kitchens and J. L. Bear, *Thermochim. Acta*, 1970, **1**, 537.
- A. Altomare, G. Cascarano, C. Giacovazzo, A. Guagliardi, M. C. Burla, G. Polidori and M. Camalli, *J. Appl. Crystallogr.*, 1994, **27**, 435.
- G. M. Sheldrick, SHELXL-97, University of Göttingen, Germany, 1997.